

Physico/Chemical Characterization, In Vitro, and In Vivo Evaluation of Hydroxyapatite/PLGA Composite and Tricalcium Phosphate Particulate Grafting Materials

Maria E. Coimbra^{1,6} / Marcos B. Salles² / Marcelo Yoshimoto² / Sergio Allegrini Jr.³ / Elizabeth Fancio⁴ / Olga Higa⁴ / Marcelo Suzuki⁵ / Paulo G. Coelho⁶

¹Department of Materials Science, Instituto Militar de Engenharia (IME), Rio de Janeiro, RJ, 22290-270, Brazil.

²Institute of Biomedical Science, University of São Paulo (USP), São Paulo, SP, Brazil.

³Department of Maxillofacial Orthopedics, Ernst-Moritz Arndt-University, Greifswald, D-17475, Germany.

⁴Institute of Materials Science, IPEN – Instituto de Pesquisas Energéticas e Nucleares, University of São Paulo, São Paulo, Brazil.

⁵Department of Prosthodontics and Operative Dentistry, Tufts University School of Dental Medicine, Boston, MA, USA.

⁶Department of Biomaterial and Biomimetics, New York University, College of Dentistry, New York, NY, 10100, USA.

Background: The purpose of this study was to physico/chemically characterize and evaluate the in vitro cytotoxicity/in vivo bone regeneration of two grafting materials in a rat calvaria model.

Materials and Methods: Two particulate grafting materials, Hydroxyapatite (HA)/PLGA (poly [L-lactide-co-glycolide]) composite (MA1) and Tricalcium Phosphate (MA2), were characterized by SEM, TEM, XRD (Rietveld), and FTIR. The cytotoxicity was evaluated by the ISO 10993-5 method. Two critical defects with 5.5 mm in diameter were created bilaterally in the calvaria of 20 Wistar rats. One defect was filled with a grafting material, and the other was the control (C, blood clot). After four and eight weeks in vivo, the amount of new bone filling the defects was evaluated using micro-computed tomography with a slice resolution of 30 μm . Statistical analysis was performed by one-way ANOVA at 95% level of significance.

Results: The physico/chemical analytical tools showed that MA1 was a Si- and Mg-doped Hydroxyapatite/PLGA composite, and MA2 was a β -TCP-based powder presenting ~9% $\text{Ca}_2\text{P}_2\text{O}_7$ secondary phase. Both powders were not cytotoxic up to 50% extract concentration. The new bone volume to total defect volume ratios at four weeks were (mean \pm SD) MA1=14.8 \pm 7.9%^a, MA2=16.1 \pm 7.2%^a, and C=6.5 \pm 1.6%^b. At eight weeks, the values were MA1=22.6 \pm 7.2%^a, MA2=19.9 \pm 4.0%^a, and C=7.4 \pm 5.2%^b.

Conclusion: Despite substantial compositional differences, non-significant differences in the amount of new bone formation were observed. Both materials presented osseointegrative properties.

Key words: grafting materials, characterization, HA/PLGA, β -TCP, in vivo, MicroCT

TITANIUM 2009 1(1): 16-28

INTRODUCTION

An important aspect of the human skeleton is its ability to regenerate itself as part of a repair process. However, depending on the size of the defect, full regeneration of the lost tissue may not occur, representing challenging scenarios for the reestablishment of organ form and function.^{1,2} In general, grafting procedures are necessary for improving the bone tissue ability to regenerate. For this purpose, several approaches have been attempted for defect filling and subsequent regeneration, including autogenous and xenogenous bone grafting and synthetic biomaterials.³

Due to its high biocompatibility, autogenous bone taken from a secondary surgical site has been widely utilized.^{4,5} However, its utilization has limitations such as supply amount and unpredictable healing kinetics. Also, donor site pain and potential post-surgical infection are common complications associated with such procedure.⁴ These limitations have stimulated the development of synthetic materials/matrices engineered specifically for bone replacement applications.^{3,4,6}

Over the last 10 years, attention has been devoted towards the development of optimized synthetic or semi-synthetic substitutes for autogenous bone grafting.¹ Commonly utilized grafting materials include allografts such as demineralized bone matrix particles, deproteinized cancellous chips, or synthetic alloplasts such as calcium sulfate pellets and porous calcium phosphate materials.³ Among alloplasts, calcium and phosphate-based substitutes have been demonstrated to have the ability to fill large defects while providing osseointegrative properties leading to new bone formation in large defects.² In addition, Ca- and P-based alloplasts may be manufactured in a variety of forms,

such as bulk ceramics, powders, and cements, and thereby may be engineered for specific applications.²

Bioceramics have been widely studied for orthopedic and dental applications due to their good biocompatible and osseointegrative properties. It has been general consensus that the bioactivity of bioceramics relies on their ability to induce hydroxyapatite (HA) formation in the physiologic environment.⁷ Commonly available resorbable bioceramics include hydroxyapatite and tricalcium phosphate powders or blends of different Ca- and P-based phases.²

Synthetic hydroxyapatite is a crystalline calcium- and phosphate-based bone substitute. However, because of slow *in vivo* resorption, hydroxyapatite-based materials have been modified by a variety of techniques in an attempt to better tailor its *in vivo* osseointegrative and dissolution properties.² Aiming to better utilize its osseointegrative properties, hydroxyapatite has also been used in blends (biphasic powders).² Alternative approaches also include the incorporation of biocompatible polymers on HA powder surfaces.⁸

Tricalcium phosphate has a faster dissolution rate than hydroxyapatite. The faster dissolution/resorption of β -TCP may allow a gradual biological degradation over a period time and a progressive replacement by the natural host tissue.⁹ Thus, β -TCP is currently considered as an alternative material for bone reconstruction and is frequently used for bone repair in the form of ceramic blocks, granules, and calcium phosphate cements.¹⁰

The purpose of this study was to physico/chemically characterize and evaluate the *in vitro* cytotoxicity and the *in vivo* bone regeneration of a Hydroxyapatite/PLGA composite and a β -tricalcium phosphate-based powder grafting material in a critical size defect.

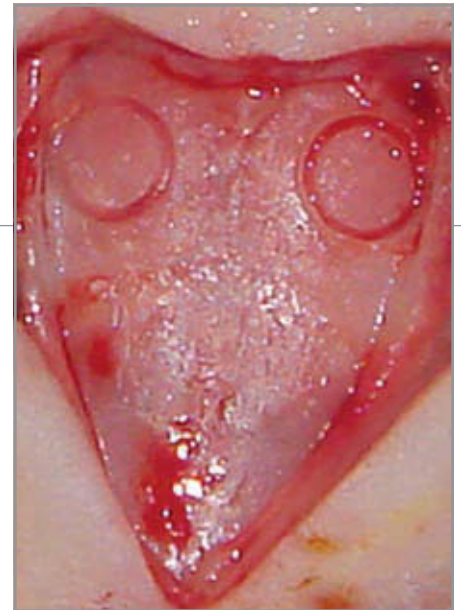


Figure 1: Skull exposure showing where the defects were made.

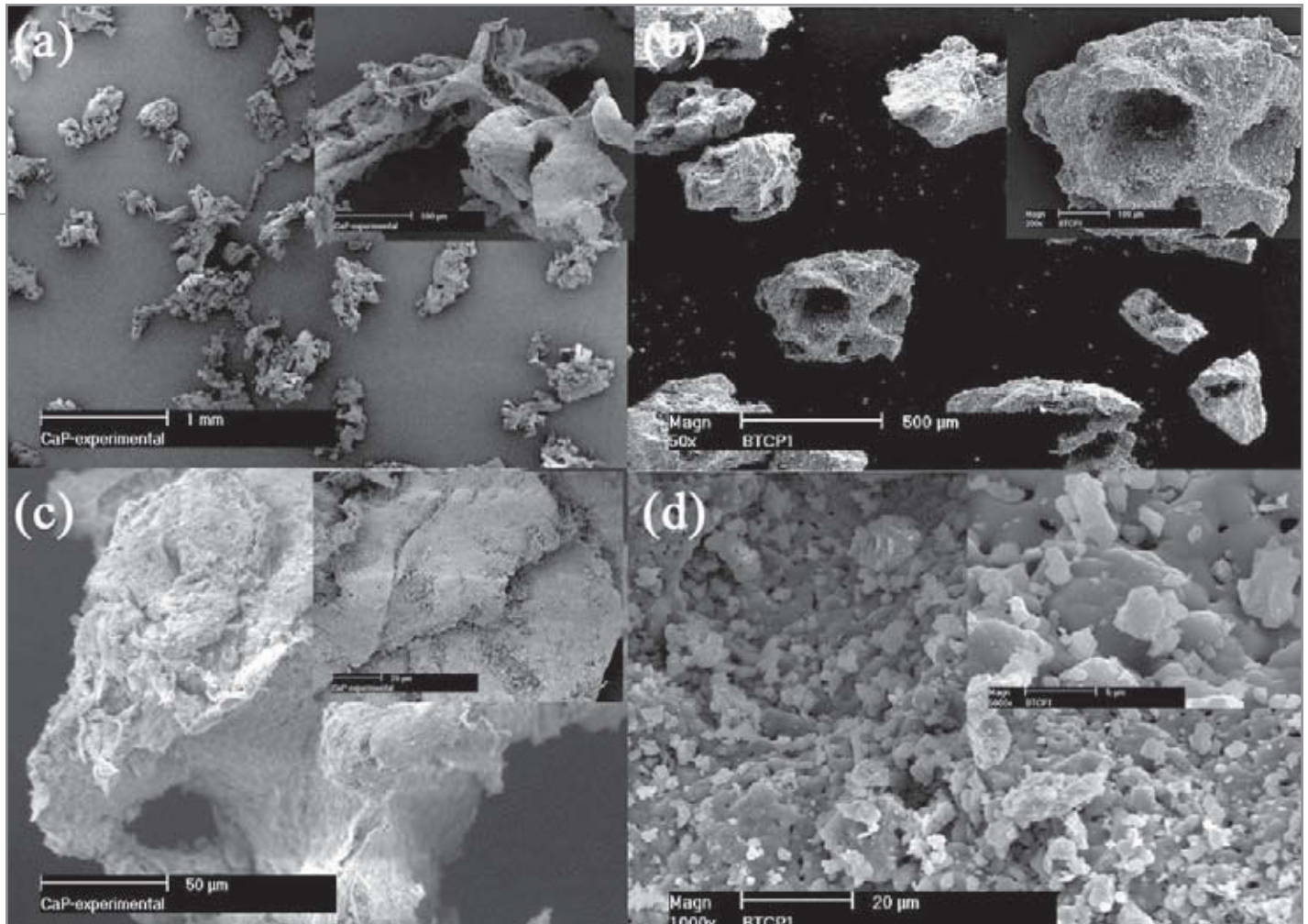


Figure 2: (a) MA1 (Hydroxyapatite/PLGA composite) powder morphology; (b) MA2 (Tricalcium Phosphate) granules morphology; (c) MA1 surface characteristic, such as roughness and porosity; (d) MA2 surface characteristic, such as roughness and porosity.

MATERIALS AND METHODS

A Hydroxyapatite (HA)/ PLGA composite particulate material— MA1 (ReOss™, Intra-Lock, Boca Raton, FL) and an FDA approved beta-tricalcium phosphate (β-TCP) – MA2 (SynthoGraft™, Bicon LLC, Boston, MA) grafting material with particle size suitable to maxillofacial applications were evaluated. The powders were provided by the manufacturers and were characterized in the as-received form without detailed disclosure of their physico/chemical characteristics.

Physico/Chemical Analysis

Powder Morphology

For particle morphology evaluation, the powders were separated in various

batches and scanning electron microscopy (SEM, Philips XL30, Eindhoven, The Netherlands) was performed at various magnifications following standard guidelines for ceramic powder imaging.

Powder Chemical Assessment

Assessment of the powder bulk composition was performed by energy dispersive spectroscopy (EDS) at various magnifications and accelerating voltages at randomly selected spots.

X-ray powder diffraction patterns (XRD) were collected in a Rigaku diffractometer (Multiflex, Tokyo, Japan), from 5° to 110° (2θ) with step interval $\Delta 2\theta = 0.02^\circ$, divergence slit = $1/2^\circ$ and receiving slit = 0.3mm, step time = 8s, 40kV, 30ma

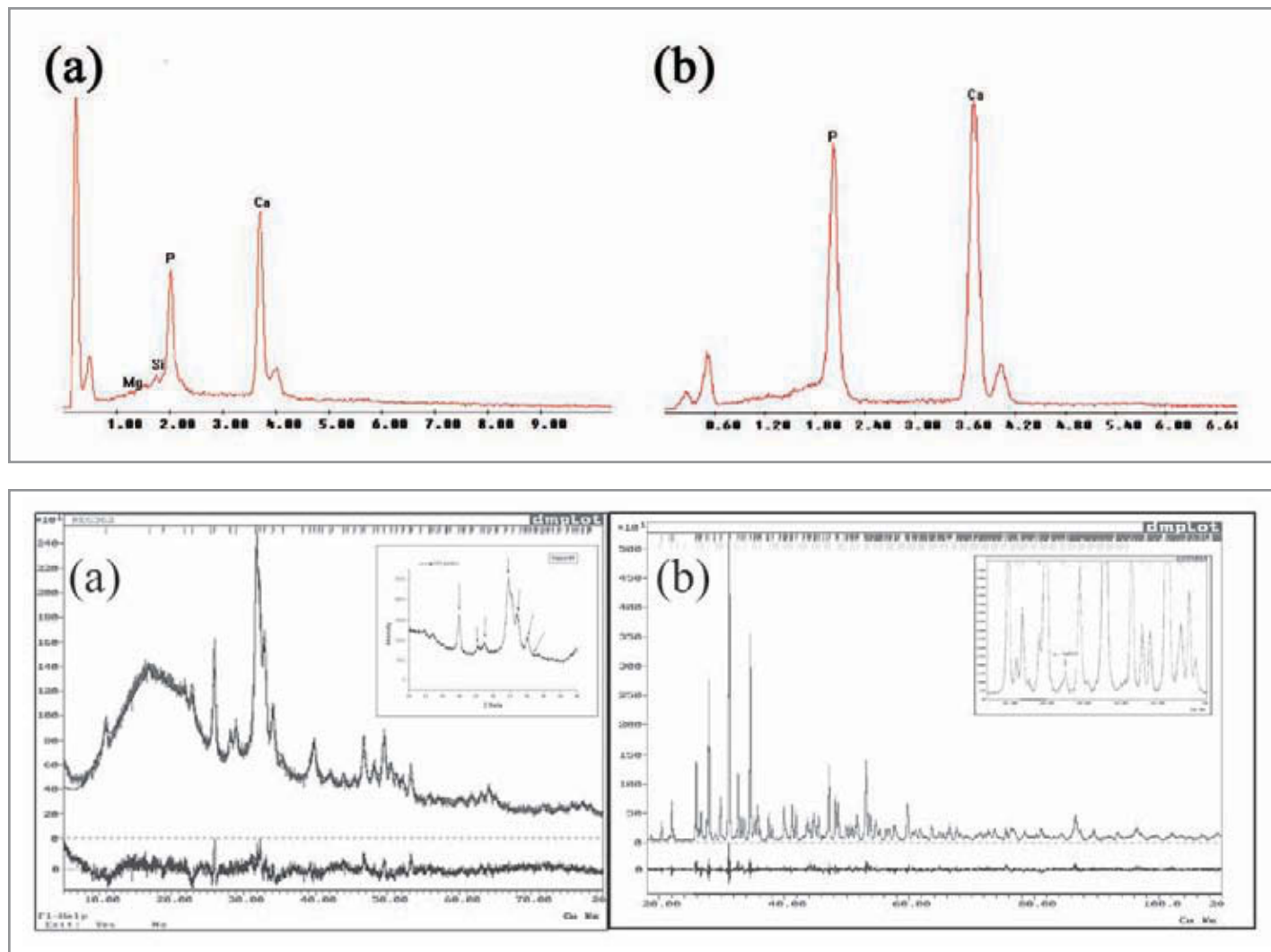


Figure 3 (Top): (a) EDS spectrum of MA1 (Hydroxyapatite/PLGA composite), and (b) EDS spectrum of MA2 (Tricalcium Phosphate).

Figure 4 (Bottom): (a) Rietveld refinement of the MA1 (Hydroxyapatite/PLGA composite) powder XRD spectrum and refinement plot results 20° to 40° 2θ spectrum showing HA peaks with broad base, typically found in non-sintered powder samples. (b) MA2 (Tricalcium Phosphate) Rietveld refinement plot results for the phases β - $\text{Ca}_3(\text{PO}_4)_2$ and β - $\text{Ca}_2\text{P}_2\text{O}_7$, and refinement plot results between 25° and 35° 2θ .

CuK_α radiation monochromatized by graphite crystal. Identification of phases was achieved by comparing the diffraction patterns obtained to the database provided by ICDD.¹¹

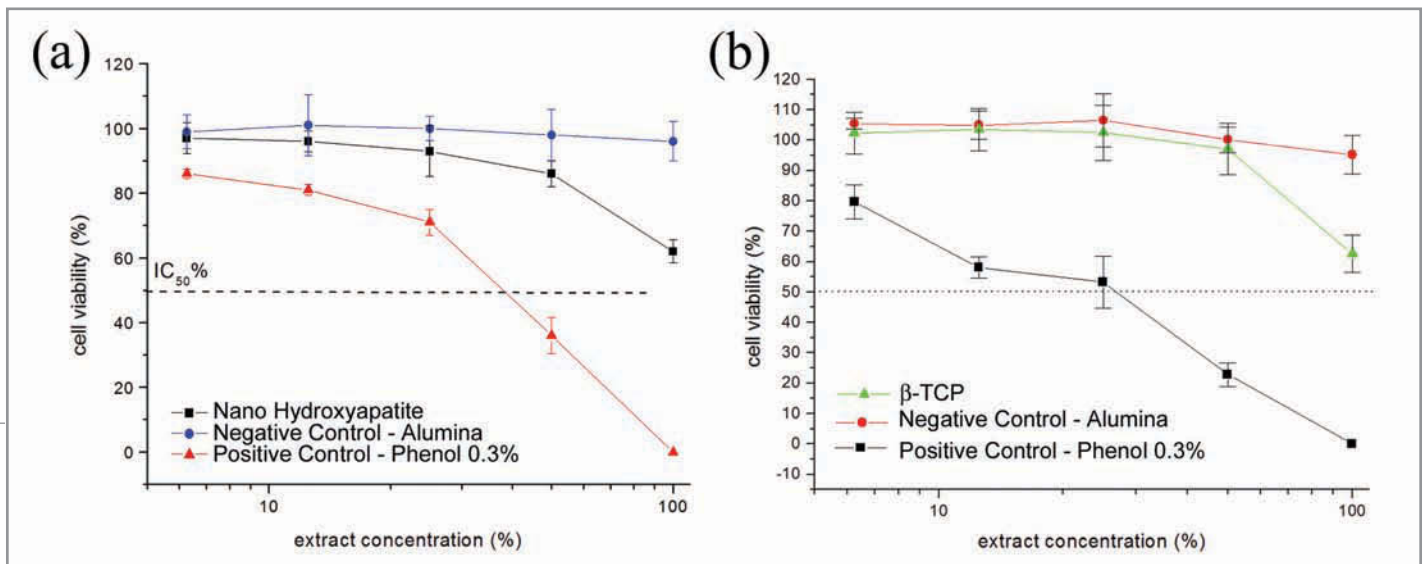
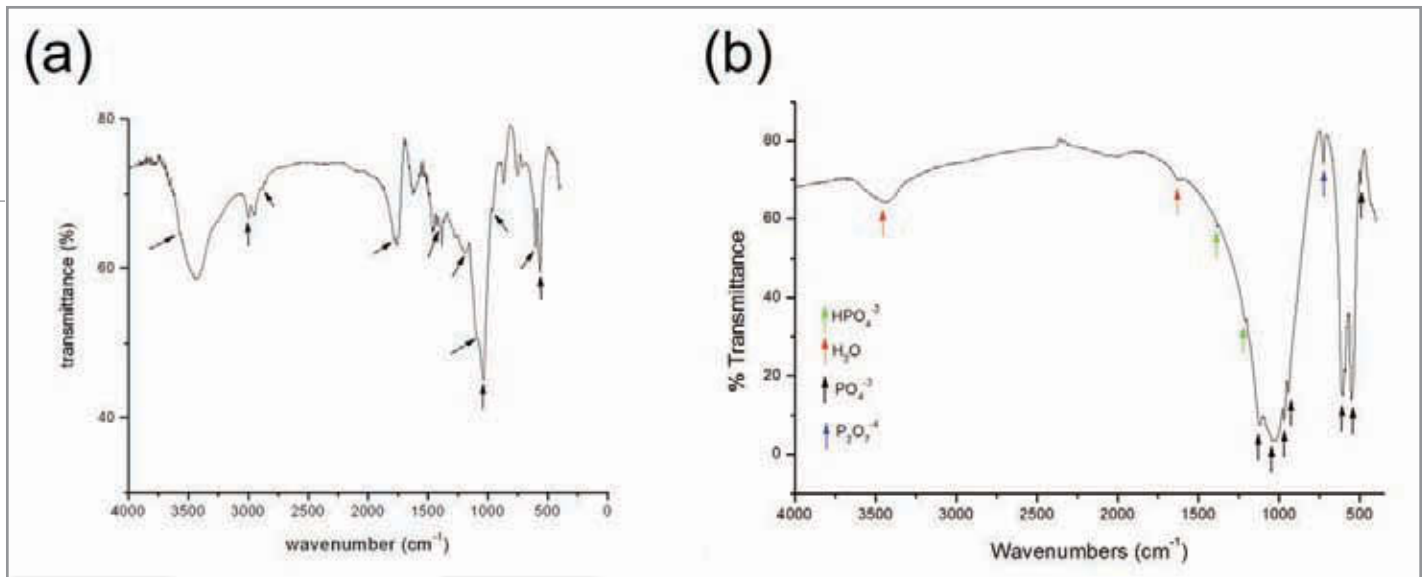
The Rietveld refinements were performed using the GSAS software Collaborative Computational Project number 14 (CCP14) in Powder and Small Molecule Single Crystal Diffraction.¹² The starting model used in the refinement was based on the theoretical structure in the Inorganic Crystal Structure Database (ICSD).¹³ The peak shapes were modeled using the pseudo-Voigt function. The background, cell parameters, preferred orientation, peak asymmetry, atomic po-

sitions, site occupancy factors, and global vibrational parameters were refined. The calculated and observed patterns were fitted by least squares method until a minimum was reached. The integrated intensities and the peak heights were related to a scale factor. The fraction of each phase was determined by the equation:

$$W_i = S_i (ZMV)_i / \sum [S_j (ZMV)_j] \quad (1)$$

Where: W_i = weight fraction of the phase p ; S = scale factor; Z = number of formula units per unit cell; M = mass of the formula unit; and V = unit cell volume.

Fourier-transform infrared spectros-



copy Magna-IR 550 Spectrometer Series II (Nicolet, Madison, WI, USA) equipped with reflectance attachment was used to determine chemical groups and crystallinity and further confirm XRD results. The spectra were collected at room temperature at a nominal resolution of 4.00 and number of sample scans equal to 1,000. The FTIR spectra were recorded in the 400–4,000 cm^{-1} range using specular reflection.

Cytotoxicity In Vitro Test

The cytotoxicity test was carried

out in order to detect toxicity levels of the as-received MA1 and MA2 powders. The employed cell line was based on the International Standards Organization ISO 10993-5 guidelines. A monolayer of cell culture of Chinese hamster ovary cells (CHO-K1 from American Type Culture Collection, ATCC) in log phase was harvested by trypsinization. The cell suspension was centrifuged and the pellets were resuspended in RPMI medium after thorough washing with sterile PBS.

One gram of each sterilized powder material was poured into 10ml glass flasks.

Figure 5 (Top): (a) FTIR spectrum for MA1 (Hydroxyapatite/PLGA composite) showing bands originating from HA, alpha-TCP phases, and PLGA component. (b) FTIR spectrum of as-received MA2 (Tricalcium Phosphate) showing bands originating from HPO_4^{2-} , H_2O , PO_4^{3-} , and $\text{P}_2\text{O}_7^{4-}$.

Figure 6 (Bottom): In vitro cytotoxicity assay employing cell culture based on the ISO 10993-5 guidelines. (a) MA1 (Hydroxyapatite/PLGA composite) cell viability level > 50% at 100% extract concentration. (b) MA2 (Tricalcium Phosphate) cell viability level > 50% at 100% extract concentration.

Four milliliters of RPMI-FCS (RPMI 1640, containing 10% fetal calf solution and 1% penicillin/streptomycin solution) culture medium was added and incubated for 48 h at 37°C under a 5% CO₂ humidified atmosphere. The supernatant was filtered through a membrane (Millipore®, Barueri, SP, Brazil), and serial dilutions (100, 50, 25, 12.5 and 6.25 vol%) were made from the

microplate was then incubated under a 5% CO₂ humidified atmosphere. After 72 h, 20 µl of a mixture (20:1) of 0.2% a supravital dye tetrazolium compound (MTS) and 0.09% of electron coupling reagent phenazine methosulfate (PMS) in PBS were added to the test wells. These were allowed to react for 2 h. The cytotoxicity test performed was based on the quantitative assessment of surviving viable cells upon exposure to a toxic agent, by incubation with the MTS compound and an electron coupling reagent PMS.

The MTS was bioreduced by cells into a formazan product that is soluble in cell culture medium. Following the release of this product, colorimetric analysis of the incorporated dye was performed. Incorporate dye was measured by reading the absorbance at 490 nm in a spectrophotometric microplate reader against a blank column.

In Vivo Experiment Animals

Twenty male Wistar rats, aged 100 days with approximately 350g body mass, were used. The animals were kept in plastic cages, maintained under a 12 h light cycle (40 lux) per day and fed *ad libitum* with sterile water and food. The surgical protocol was approved by the Animal Care Committee of the University of São Paulo, São Paulo, Brazil. The animals were maintained at the IPEN animal facility.

Surgical Procedures

Two critical defects with 5.5 mm in diameter were created bilaterally in the calvaria (Fig. 1) and were allowed to heal for periods of four and eight weeks. One defect was filled with one of the grafting materials and the other was the control (C, blood clot, Table 1).

All animals were submitted to calvaria surgery under general anesthesia.

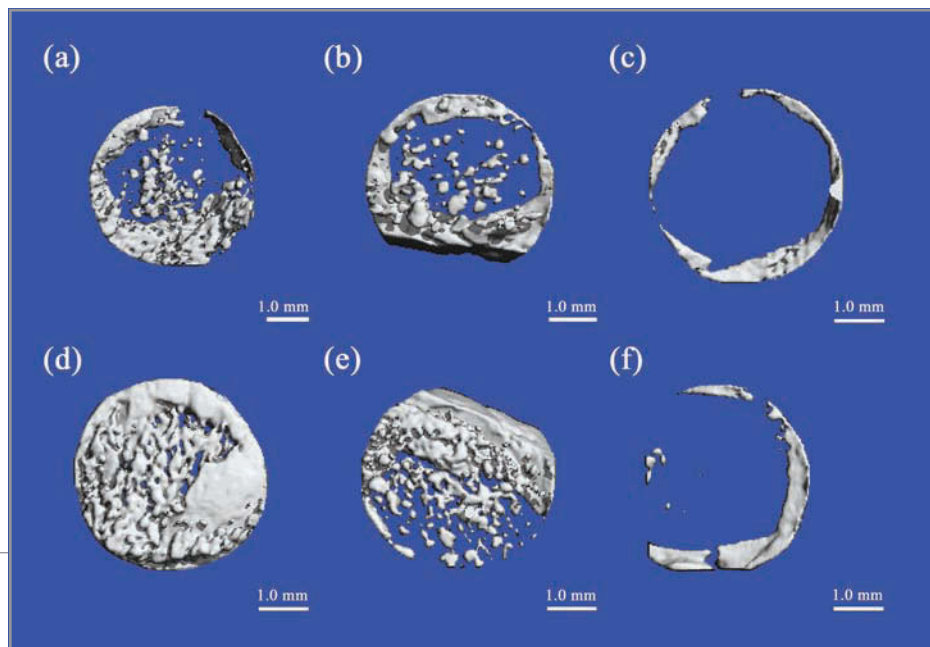


Figure 7: μ CT 3D reconstruction after four weeks of healing: (a) MA1 (Hydroxyapatite/PLGA composite), (b) MA2 (Tricalcium Phosphate), (c) Control; and after eight weeks of healing: (d) MA1 (Hydroxyapatite/PLGA composite), (e) MA2 (Tricalcium Phosphate), (f) Control.

extract. Dilutions were also performed for the negative and positive material controls, which were sterile alumina ceramic and 0.02 vol% phenol solutions, respectively. All concentrations were tested in quadruplicate.

A 96-well tissue culture microtiter plate was prepared by pipetting 50 µL of the serial dilutions of each extract. The plate was brought to equilibrium at 37°C in a humidified atmosphere under 5% CO₂ while the cells were harvested for assay. Subsequently, 50 µL of the cell suspension (~3,000 cells) was dispensed into each well. The resulting volume in each well was 100 µL. Control columns of four wells were prepared with medium without cells (blank) and medium plus cells without extract (100% survival). The

For sedation and muscle relaxation, each animal received an intraperitoneal injection (2-(2-xylidine)-5,6-dihydro-4H-1,3-thiazyn chlorate (Rompum, Bayer; São Paulo, SP, Brazil) (5.0mg/kg). For general anesthesia, ketamine (Ketamina®, Agener; União Química Farmacêutica Nacional SA, São Paulo, SP, Brazil) (60mg/Kg) in proportion 2:1 was administered. Throughout the surgical procedure, the animals were maintained at deep anesthesia for 40 minutes. Prior to shaving by a surgical blade, the frontoparietal region was scrubbed with povidone iodine 10% in aqueous solution with 1% of active iodine (PVPI).

A 15mm long mid-sagittal full-thickness incision was made with a #15 surgical blade to expose the skull. The skin, muscles, and periosteum were reflected to expose the parietal bones. By means of a surgical trephine bur of 5.5 mm diameter, a perforation crossing the parietal's bone entire diploe exposed the dura mater at the bottom of the defect under constant irrigation with sterile saline solution (Fig. 1). The defect was filled with the grafting materials according to Table 1. The control defect was allowed to fill with blood clot. The tissues were closed in layers with 4-0 Dexon sutures (Ethicon, Sommerville, NJ, USA), and 4-0 vicryl sutures (Hu-Friedy, Chicago, IL, USA).

After four and eight weeks post-surgery, euthanasia was performed with CO₂ inhalation for 10 minutes. After euthanasia, the crania were carefully dissected free of soft tissue and the skullcaps were collected and fixed in 4% buffered formalin for 24 hours. After fixation, the samples remained in 70% ethanol.

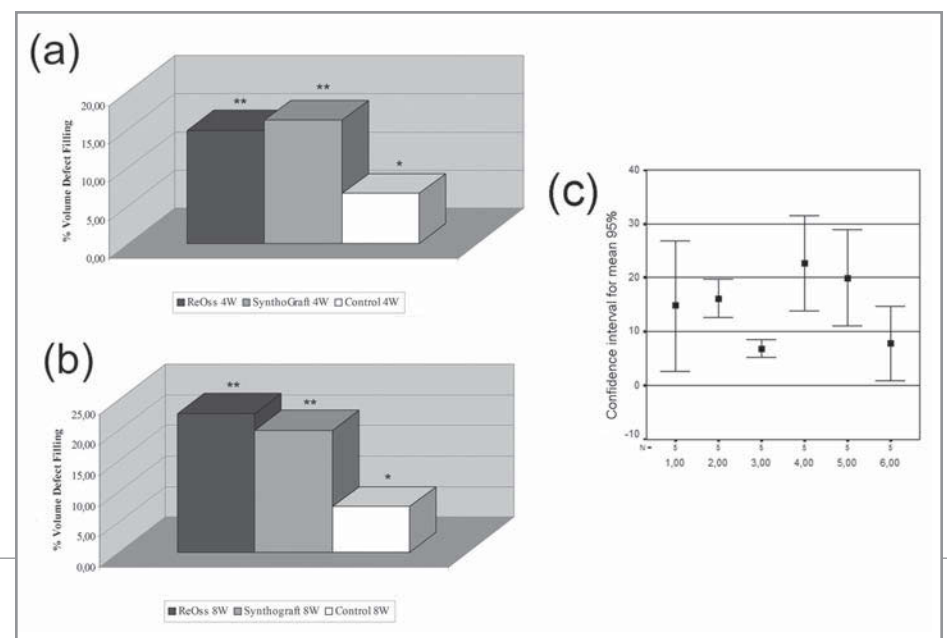
Micro Computed Tomography

The amount of bone filling the defects was examined using micro computed tomography (μ CT 40, Scanco Medical, Basserdorf, Germany) with a slice resolu-

tion of 30 μ m. Five hundred and seven μ CT slices were imaged at the skull caps at an X-ray energy level of 70 kVp, and a current of 114 μ A. Integration time was 150 ms with a total scanning time of 19.8 min (78mAs). The 3D construction of the calvaria bone was made using a template restricted to the defect margins.

Statistical Analysis

Statistical analysis was performed by one-way ANOVA at 95% level of significance and multiple comparisons were performed by Tukey's post-hoc.



RESULTS

Physico/Chemical Analysis Powder Morphology

Irregular powder morphology was observed for the MA1 (Figs. 2a and 2c). Figures 2b and 2d depict the irregular morphology for the MA2 particles. Intragranular porosity could be observed at the ceramic bulk for the MA2 powder, revealing that the granules were subjected to a sinterization process or a thermal treatment and were subsequently milled to the final powder form. Other observations

Figure 8: Mean bone fill percentages in 5.5 mm parietal defect filled with MA1 (Hydroxyapatite/PLGA composite), MA2 (Tricalcium Phosphate), and blood clot. (a) After four weeks of healing. (b) After eight weeks of healing and (c) means \pm standard deviations for the different in vivo groups (1 – ReOss 4W; 2 – SynthoGraft 4W; 3 – Control 4W; 4 – ReOss 8W; 5 – SynthoGraft 8W; 6 – Control – 8W).

TABLE 1: MATERIALS AND SURGICAL GROUPS DIVISION

Groups	N	Description
MA1-4 Weeks	5	5 MA1*
		5 Control (Blood Clot)
MA2-4 Weeks	5	5 MA2**
		5 Control (Blood Clot)
MA1-4 Weeks	5	5 MA1
		5 Control (Blood Clot)
MA2-4 Weeks	5	5 MA2
		5 Control (Blood Clot)

Legend: * MA1 – Hydroxyapatite PLGA composite / ** MA2 – Tricalcium Phosphate

included a range of particle size for both powders and particle porous morphology.

Powder Chemical Assessment

Within the EDS interaction/detection volume, the spectrum showed that both powders were initially free of contamination. The MA1 EDS spectrum showed the presence of Ca, P, Si, and Mg (Fig. 3a), while the MA2 spectrum showed only calcium and phosphorous peaks (Fig. 3b).

The XRD results for both powders showed peaks related to biocompatible Ca- and P-based phases. The XRD spectra presented in Figure 4a showed the absence of phases secondary to HA for the MA1 powder. During the refinement for the MA1 sample, the background was defined manually since the data was collected without a pattern and the amorphous percentage obtained was high for polynomial definition. However, further spectrum refinement was difficult due to the high background resulting from the polymeric organic content. Further investigation of the spectrum at the region ranging from 20° to 40° 2θ (Fig. 4a)

showed that the peaks presented a broad base compared to dense, sintered, crystalline HA (Fig. 4a).

For the β -TCP, the final Rietveld plot presented in Figure 4b displayed reasonable agreement between the structural model and the raw data. In general, the X-ray patterns collected for calcium phosphates have a great number of superimposed peaks. The Rietveld method resolved the peaks for the quantitative analysis even for low phase's percentages. Figure 4b depicts the most intense Bragg reflection for β - $\text{Ca}_2\text{P}_2\text{O}_7$, according to ICDD data base 9-346, which was identified, and the quantitative analysis for this phase could be determined at approximately 9% (Table 2).

The infrared spectra further confirmed the XRD findings for both powders, and are presented in Figure 5. The FTIR spectrum of MA1 (Fig. 5a) showed bands characteristic of HA and one minor β -TCP band, along with bands related to the PLGA polymer. The various bands chemical groups are presented as follows: Band (in cm^{-1}), 3572 – OH-HA; 2998

– C-H-CH₃; 2883 – C-H-CH₂; 1400 – CO₃-Carbonate, minor; 1187 – C-O; 1087 – ν_3 PO₄; 1039 – Si-O-Si or 1040 – PO₄; 960 – ν_1 PO₄; 601 – ν_4 PO₄; and 563 – α -TCP.

For the MA2 powder, the absence of 460 and 740 cm^{-1} bands and of an isolated band approximately at 600 cm^{-1} characteristic of the α -TCP confirmed the XRD and Rietveld refinement findings. A characteristic of this calcium phosphate is a wide band from 900 to 1,200 cm^{-1} .³⁰ The band at 1,650 cm^{-1} was assigned to adsorbed H₂O. The absorption bands at 1,092; 1,044; 1,036; 960; 602; 573; and 475 cm^{-1} were assigned to the vibration in the PO₄³⁻ group. The presence of a peak at 725 cm^{-1} is characteristic of the symmetric mode $\nu(\text{P-O-P})$ P₂O₇⁴⁻. The characteristic peak at 1,211 cm^{-1} refers to the non degenerate flat deformation of hydrogen in groups: ${}^3\text{OPO-H}---\text{O-PO}_3$, common in HPO₄²⁻ ions. This is related to the water molecule interaction in the crystalline net (Fig. 5b).

Cytotoxicity In Vitro Test

The cytotoxicity evaluation data obtained for the different extract concentrations of the powders, negative and positive, material controls is presented in Figure 6. These values are related to the cell viability at different extract concentrations.

The index of cytotoxicity ($\text{IC}_{50(\%)}$) is the concentration of the extract necessary to kill half of the cell population. The negative control (alumina) did not exhibit any cytotoxicity effect ($\text{IC}_{50(\%)} \sim 100$). In contrast, the positive control (phenol solution 0.02 vol %) demonstrated high cytotoxicity levels ($\text{IC}_{50(\%)} \sim 0$). The powders tested did not show any cytotoxicity effect up to 50% extract concentration, where its $\text{IC}_{50(\%)}$ presented comparable values relative to the negative control. At 100% extract concentration the $\text{IC}_{50(\%)}$ decreased to ~ 65 for both materials.

TABLE 2: RIETVELD REFINEMENT RESULTS FOR HYDROXYAPATITE/PLGA COMPOSITE AND TRICALCIUM PHOSPHATE SAMPLES

Sample	MA1-Hydroxyapatite HA	MA-2 Tricalcium Phosphate β -TCP	β -Ca ₂ P ₂ O ₇
a (Å)	9.437±0.000	10.425±0.000	6.689±0.000
b (Å)	9.437±0.000	10.425±0.000	6.689±0.000
c (Å)	6.879±0.000	37.414±0.009	24.152±0.036
V(Å ³)	530.80(1)	3521.4±0.2	1080.6±0.2
d(g.cm ³)	3.150	3.130	3.125
*R _{WP}	7.31	11.93	11.93
*S	1,82	1,51	1,51
*R _B	12,36	5.40	5.50
% mass	100.0	91.04±0.69	8.96±0.86

*R and S indexes are defined in Young & Wiles³⁵

In Vivo Results

The in vivo results showed that both powder materials were biocompatible, osseoconductive, and presented the ability to provide physical support for bone in-growth for the implantation times investigated. Qualitative analysis showed that newly formed bone was in continuity with the host cortical and trabecular bone structure for both materials and times in vivo.

After four weeks of healing, MA1 and MA2 presented bone formation located primarily at the central region and the margins of the defect (Figs. 7a and 7b). After eight weeks, both materials presented higher amounts of bone regeneration throughout the critical defect (Figs. 7d and 7e). As observed at the 3D reconstructions, the materials appeared to act as bridges for the bone formation.

The new bone volume to total defect volume ratios at four weeks were (mean ± SD) MA1=14.8 ± 7.9%^a,

MA2=16.1 ± 7.2%^a, and Control=6.5 ± 1.6%^b. At eight weeks, increased values were observed for both materials, MA1=22.6 ± 7.2%^a, MA2=19.9% ± 4.0%^a, and Control=7.43±5.23%^b (experimental groups non significant compared to four weeks, Fig. 8).

DISCUSSION

In agreement with previous studies testing HA/PLGA composite and TCP-based particulate materials, the in vitro and in vivo results obtained for both powders supported their biocompatible and osseoconductive physico/chemical properties suitable for bone regeneration.¹⁴⁻¹⁷ The series of physico/chemical analytical results, which showed powders of Ca- and P- based composition of crystalline phases (primarily HA-based and β -TCP-based) known to present bioactive properties without non biocompatible contaminants, supported the favorable results obtained in the in vitro

cytotoxicity assessment and in vivo new bone formation.

The particle morphologies observed for both powders were representative of powder shapes and size range utilized for maxillofacial bone regeneration.⁸ The irregular shapes observed for MA1 and MA2 provided both materials packability on the critical defects created in the rats' skulls. However, due to the presence of the polymer component in MA1, its placement, shaping, and initial stability was more easily achieved.

Although both β -TCP and HA powders are considered suitable materials for bone regeneration procedures,^{9,10} the optimal powder composition and morphology that will render rapid bone formation in tandem with a gradual temporal dissolution of the powder material for varied applications has been a source of speculation for a number of years.^{18,19}

According to the literature,^{14,20,21} due to its primary composition, the MA2

powder will present a substantially higher dissolution rate compared to MA1. In addition to the higher dissolution rate compared to pure crystalline HA powders, the presence of approximately 9% of a secondary phase on MA2 will further accelerate its initial powder dissolution.¹⁵

When considering the possible routes for β -TCP synthesis:

$$2\text{CaHPO}_4 \cdot 2\text{H}_2\text{O} + \text{Ca}_{10}(\text{PO}_4)_6(\text{OH})_2 \Rightarrow 2\text{Ca}_3(\text{PO}_4)_2 + 2\text{Ca}_2\text{P}_2\text{O}_7 + 2\text{CaO} + 6\text{H}_2\text{O}$$

or $\text{Ca}_{10-x}(\text{HPO}_4)_x(\text{PO}_4)_{6-x}(\text{OH})_{2-x}$ ($\text{Ca}/\text{P}=1,50$) $\Rightarrow 2\text{Ca}_3(\text{PO}_4)_2 + \text{Ca}_2\text{P}_2\text{O}_7 + \text{CaO} + \text{H}_2\text{O}$, the presence of a low percentage of $\text{Ca}_2\text{P}_2\text{O}_7$ is expected.²²

While there are concerns regarding the presence of $\text{Ca}_2\text{P}_2\text{O}_7$ resulting in a dissolution rate that is too fast for bone formation while maintaining appropriate physical integrity,²² it has been speculated that the rapid release of Ca and P at the material surface may be beneficial for the early stages of wound healing.²² The potential benefits may arise from the large availability of bioactive elements at the material for surface biomineralization and the stimulation of osteoclasts, and the potential phenotypic differentiation of the osteogenic cells.²²

On the other hand, it has also been demonstrated that HA powders will present a dissolution rate that may be too slow for total powder material resorption to occur, possibly resulting in the presence of HA particles for extended periods of time after implantation.²³ For this purpose, modifications such as the interplay between its macro and micro porosity, blending HA powder with other Ca- and P-based phases of faster dissolution, elemental chemistry alteration, and application of polymeric materials have been attempted.^{24,25}

Compared to β -TCP, slower dissolution and bone remodeling is expected

to occur for the MA1 powder. However, unlike commonly observed HA powders utilized for maxillofacial purposes, the Si and Mg content along with the presence of a PLGA in formulation of MA1 may result in significantly different *in vivo* behavior compared to a pure crystalline HA powder. Si and Mg are known to occupy the different sites of the HA lattice, and in reduced quantities have been shown to increase bioactive ceramics' osseointegrative properties²⁵ without substantially altering their dissolution behavior. On the other hand, the presence of PLGA, which is a blend of polylactic acid (PLA) and polyglycolic acid (PGA), will dynamically change the initial healing kinetics around the grafted material.^{26,27}

The final products of the biopolymers degradation may positively affect the host to biomaterial temporal response. Immediately following implantation, the dissolution of biopolymers such as PLGA will generate the hydrolytic release of acids related to the citric acid cycle. After the hydrolysis, the degradation follows an oxidation process, transforming PLA in lactic acid and PGA in glycine and pyruvic acid. In the presence of acetyl CoA, CO_2 is released and decomposition of PLA and PGA subproducts to citrate occurs. The citrate is then incorporated at the citric acid cycle, resulting in CO_2 and H_2O , which can be excreted by urine and/or by the lungs.^{27,28} Thus, through the course of the biopolymer degradation, the acidic environment generated during the degradation of the PLGA content may increase the amount of Ca and P released from the HA particles, possibly resulting in an auto-catalytic path as the MA1 particles are dissolved, exposing more PLGA from the particle microstructure.

The cytotoxicity assay showed slight cytotoxic levels for both materials after the extract concentration increase. However, such slight *in vitro* cytotoxic at

high extract concentrate values did not result in adverse effects at the tissue level since bone regeneration was observed for both materials in the rat calvaria model.

Over the last few years, μCT has been used to quantitatively investigate the 3D trabecular bone structure in physiological or pathological environment.²⁹ In several studies, μCT results highly correlated to those obtained with conventional histology for imaging and quantification of trabecular bone structure on human bone biopsies and animal trabecular bone.^{30,31}

Although the temporal amount of newly formed bone was not significantly different among and between the materials observed, the spatial distribution of newly formed bone between groups was similar showing that, despite physicochemical differences, both materials were biocompatible and osseointegrative.^{18,19} Also, a temporal increase in the amount of bone in the critical defects increased for both materials.

At four weeks implantation time, higher amounts of bone formation were observed for MA2 compared to MA1, whereas at eight weeks, higher amounts were observed for MA1, although no significant differences in the amounts of bone formation were observed at both times *in vivo*. We speculate that the result obtained at four weeks was due to the higher dissolution properties presented by the β -TCP-based powder along with the more intense initial inflammatory process due to the MA1 biopolymeric component which possibly resulted in a foreign body reaction inflammatory response.^{32,33} However, while the μCT imaging provided insight concerning the critical size defect healing between MA1 and MA2, future studies evaluating the temporal tissue and cellular level events during wound healing through histology are recommended.

CONCLUSION

This study comprised the characterization, and the *in vitro* and *in vivo* biocompatibility evaluation of a hydroxyapatite/PLGA composite and a β -TCP bone grafting particulate materials. Despite the substantial compositional differences determined by the physico/chemical characterization, non-significant differences in the amount of new bone formation were observed between materials.

ACKNOWLEDGMENTS

This research was partly supported by the Department of Biomaterials and Biomimetics, New York University, College of Dentistry. Dr. Sergio Allegri Jr. thanks the Alexander von Humboldt Foundation. The authors would also like to acknowledge the invaluable importance and assistance of the IPEN animal facility.

REFERENCES

- Marins LV, Cestari TM, Sottovia AD, Granjeiro JM, Taga R. Radiographic and histological study of perennial bone defect repair in rat calvaria after treatment with blocks of porous bovine organic graft material. *J Appl Oral Sci* 2004;2004:62-69.
- De Long WG, Jr., Einhorn TA, Koval K, McKee M, Smith W, Sanders R et al. Bone grafts and bone graft substitutes in orthopaedic trauma surgery. A critical analysis. *J Bone Joint Surg Am* 2007;89:649-658.
- Gadzag AR, Lane JM, Glaser D, Forster RA. Alternative to autogenous bone graft: efficacy and indication. *J Am Acad Orthop Surg* 1995;3:1-8.
- Summers BN, Eisenstein SM. Donor site pain from the ilium. A complication of lumbar spine fusion. *J Bone Joint Surg Br* 1989;71:677-680.
- Aaboe M, Pinholt EM, Hjorting-Hansen E. Healing of experimentally created defects: a review. *Br J Oral Maxillofac Surg* 1995;33:312-318.
- Devin J, Attawia M, Laurencin CT. Developmental 3-dimensional polymer for bone repair. *J Biomed Sci* 1996;661-669.
- Fujibayashi S, Neo M, Kim HM, Kokubo T, Nakamura T. A comparative study between *in vivo* bone ingrowth and *in vitro* apatite formation on Na₂O-CaO-SiO₂ glasses. *Biomaterials* 2003;24:1349-1356.
- Kim SS, Ahn KM, Park MS, Lee JH, Choi CY, Kim BS. A poly(lactide-co-glycolide)/hydroxyapatite composite scaffold with enhanced osteoconductivity. *J Biomed Mater Res A* 2007;80:206-215.
- Lu J, Descamps M, Dejou J, Koubi G, Hardouin P, Lemaître J et al. The biodegradation mechanism of calcium phosphate biomaterials in bone. *J Biomed Mater Res* 2002;63:408-412.
- Descamps M, Duhoo T, Monchau F, Lu J, Hardouin P, Hornez JC et al. Manufacture of macroporous β -tricalcium phosphate bioceramics. *Journal of the European Ceramic Society* 2008;28:149-157.
- ILCFD. Powder Diffraction File Database. Campus Boulevard Newtown Square, PA, U.S.A.; 1995.
- (CCP14) GsCCPN. Powder and Small Molecule Single Crystal Diffraction; 1994.
- Inorganic Crystal Structure Database (ICSD). U.K.; 1995.
- Hench LL, Wilson J. An Introduction to Bioceramics. Advanced Series in Ceramics. Singapore: World Scientific Publishing Co. Pte. Ltd; 1993.
- Kokubo T, Kim HM, Kawashita M. Novel bioactive materials with different mechanical properties. *Biomaterials* 2003;24:2161-2175.
- Jensen SS, Yeo A, Dard M, Hunziker E, Schenk R, Buser D. Evaluation of a novel biphasic calcium phosphate in standardized bone defects: a histologic and histomorphometric study in the mandibles of minipigs. *Clin Oral Implants Res* 2007;18:752-760.
- Walsh WR, Vizesi F, Michael D, Auld J, Langdown A, Oliver R et al. Beta-TCP bone graft substitutes in a bilateral rabbit tibial defect model. *Biomaterials* 2008;29:266-271.
- Vaccaro AR, Chiba K, Heller JG, Patel T, Thalgott JS, Truumees E et al. Bone grafting alternatives in spinal surgery. *Spine J* 2002;2:206-215.
- Meynet J. Osteotomie tibiale de valgisation par ouverture interne: place des substituts osseux. *Ann Orthopediques de L'Ouest* 1998;30: 171-173.
- Fulmer MT, Ison IC, Hankermayer CR, Constantz BR, Ross J. Measurements of the solubilities and dissolution rates of several hydroxyapatites. *Biomaterials* 2002;23:751-755.
- Chen ZF, Darvell BW, Leung VW. Hydroxyapatite solubility in simple inorganic solutions. *Arch Oral Biol* 2004;49:359-367.
- Gaasbeek RD, Toonen HG, van Heerwaarden RJ, Buma P. Mechanism of bone incorporation of beta-TCP bone substitute in open wedge tibial osteotomy in patients. *Biomaterials* 2005;26:6713-6719.
- Lopes MA, Santos JD, Monteiro FJ, Ohtsuki C, Osaka A, Kaneko S et al. Osteocompatibility and *in vivo* evaluation of glass reinforced hydroxyapatite composite. *Bioceramics* 1999;12:421-424.
- Kumta PN, Sfeir C, Lee DH, Olton D, Choi D. Nanostructured calcium phosphates for biomedical applications: novel synthesis and characterization. *Acta Biomater* 2005;1:65-83.
- Kim SR, Lee JH, Kim YT, Riu DH, Jung SJ, Lee YJ et al. Synthesis of Si, Mg substituted hydroxyapatites and their sintering behaviors. *Biomaterials* 2003;24:1389-1398.
- Middleton JC, Tipton AJ. Synthetic biodegradable polymers as orthopedic devices. *Biomaterials* 2000;21:2335-2346.
- Peltoniemi H, Ashammakhi N, Kontio R, Waris T, Salo A, Lindqvist C et al. The use of bioabsorbable osteofixation devices in craniomaxillofacial surgery. *Oral Surg Oral Med Oral Pathol Oral Radiol Endod* 2002;94:5-14.
- Ali SA, Zhong SP, Doherty PJ, Williams DF. Mechanisms of polymer degradation in implantable devices. I. Poly(caprolactone). *Biomaterials* 1993;14:648-656.
- Gauthier O, Muller R, von Stechow D, Lamy B, Weiss P, Bouler JM et al. *In vivo* bone regeneration with injectable calcium phosphate biomaterial: a three-dimensional micro-computed tomographic, biomechanical and SEM study. *Biomaterials* 2005;26:5444-5453.
- Muller R, Rueggegger P. Micro-tomographic imaging for the nondestructive evaluation of trabecular bone architecture. *Stud Health Technol Inform* 1997;40:61-79.
- Muller R, Van Campenhout H, Van Damme B, Van Der Perre G, Dequeker J, Hildebrand T et al. Morphometric analysis of human bone biopsies: a quantitative structural comparison of histological sections and micro-computed tomography. *Bone* 1998;23:59-66.
- Chu CC. Biodegradable Polymeric Biomaterials: An Update Overview. In: Bronzino J, editor. *The Biomedical Engineering Handbook*. Boca Raton, FL: CRC Press; 1999. p. cap. 41.
- Sung HJ, Meredith C, Johnson C, Galis ZS. The effect of scaffold degradation rate on three-dimensional cell growth and angiogenesis. *Biomaterials* 2004;25:5735-5742.
- Coimbra MER. Degradation of polylactide acid, bioglass and hydroxyapatite: An *in vitro* and *in vivo* study. Department of Material Science. Rio de Janeiro: Military Institute of Engineering - IME; 2008. p. 212.
- Young RA. *IU Monographs on Crystallography - 5 The Rietveld Method*. New York: Oxford University Press; 1995.

